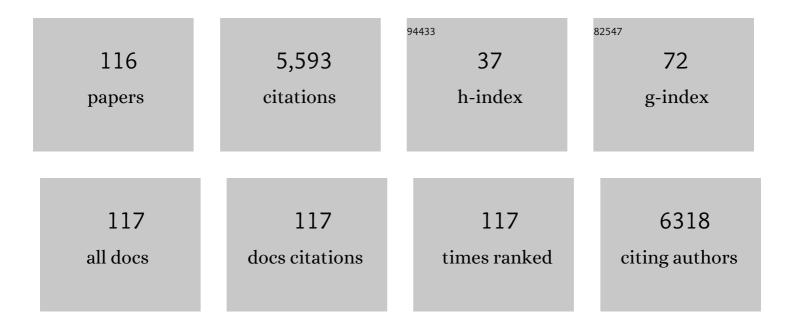
List of Publications by Year in descending order

Source: https://exaly.com/author-pdf/827553/publications.pdf Version: 2024-02-01



Ιμανι-Ιτίν Υλης

#	Article	IF	CITATIONS
1	The photothermal effect enhance visible light-driven hydrogen evolution using urchin-like hollow RuO2/TiO2/Pt/C nanomaterial. Journal of Alloys and Compounds, 2022, 890, 161722.	5.5	11
2	Enhancing the photocatalytic activity of defective titania for carbon dioxide photoreduction <i>via</i> surface functionalization. Catalysis Science and Technology, 2022, 12, 509-518.	4.1	15
3	Cis-9-Octadecenylamine modified ferric oxide and ferric hydroxide for catalytic viscosity reduction of heavy crude oil. Fuel, 2022, 322, 124159.	6.4	4
4	Synthesis of a Defective WO <sub>3–<i>y</i></sub> /TiO <sub>2–<i>x</i></sub> Composite Catalyst for Photocatalytic CO <sub>2</sub> Highly Selective Reduction. Energy & Fuels, 2022, 36, 11515-11523.	5.1	9
5	Anchoring Ni single atoms on sulfur-vacancy-enriched ZnIn2S4 nanosheets for boosting photocatalytic hydrogen evolution. Journal of Energy Chemistry, 2021, 58, 408-414.	12.9	93
6	Spatially Separating Redox Centers and Photothermal Effect Synergistically Boosting the Photocatalytic Hydrogen Evolution of ZnIn <sub>2</sub> S <sub>4</sub> Nanosheets. Small, 2021, 17, e2006952.	10.0	68
7	Rivet-like iron oxide nanoparticles and their catalytic effect on extra heavy oil upgrading. Fuel, 2021, 293, 120458.	6.4	11
8	Interfacial dual vacancies modulating electronic structure to promote the separation of photogenerated carriers for efficient CO2 photoreduction. Applied Surface Science, 2021, 551, 149305.	6.1	13
9	Sandwich-like Z-scheme g-C3N4/reduced graphene oxide@TiO2composite for enhanced visible light photoactivity. Materials Research Bulletin, 2021, 140, 111292.	5.2	4
10	Theoretical Insight into the Role of Defects and Facets in the Selectivity of Products in Water Oxidation over Bismuth Vanadate (BiVO <sub>4</sub> ). ACS Sustainable Chemistry and Engineering, 2020, 8, 1980-1988.	6.7	15
11	Facile fabrication of ZnIn2S4/SnS2 3D heterostructure for efficient visible-light photocatalytic reduction of Cr(VI). Chinese Journal of Catalysis, 2020, 41, 200-208.	14.0	100
12	Boosting visible-light-driven catalytic hydrogen evolution <i>via</i> surface Ti <sup>3+</sup> and bulk oxygen vacancies in urchin-like hollow black TiO <sub>2</sub> decorated with RuO <sub>2</sub> and Pt dual cocatalysts. Catalysis Science and Technology, 2020, 10, 7914-7921.	4.1	18
13	Construction of 2D/2D TiO2/g-C3N4 nanosheet heterostructures with improved photocatalytic activity. Materials Research Bulletin, 2020, 125, 110765.	5.2	39
14	Highly efficient photocatalytic reduction of CO2 on amine-functionalized Ti-MCM-41 zeolite. Journal of Nanoparticle Research, 2020, 22, 1.	1.9	9
15	Space-induced charge carriers separation enhances photocatalytic hydrogen evolution on hollow urchin-like TiO2 nanomaterial. Journal of Alloys and Compounds, 2020, 837, 155547.	5.5	17
16	Enhanced Photoelectrochemical Performance of g-C <sub>3</sub> N <sub>4</sub> /tiO <sub>2</sub> Heterostructure by the Cooperation of Oxygen Vacancy and Protonation Treatment. Journal of the Electrochemical Society, 2020, 167, 066513.	2.9	6
17	Oxygen Evolution Reaction (OER) on Clean and Oxygen Deficient Low-Index SrTiO <sub>3</sub> Surfaces: A Theoretical Systematic Study. ACS Sustainable Chemistry and Engineering, 2019, 7, 15346-15353.	6.7	16
18	Effect of heterojunctions and phase-junctions on visible-light photocatalytic hydrogen evolution in BCN-TiO2 photocatalysts. Chemical Physics Letters, 2019, 727, 11-18.	2.6	20

#	Article	IF	CITATIONS
19	Boosting Visible-Light Photocatalytic Hydrogen Evolution with an Efficient CuInS <sub>2</sub> /ZnIn <sub>2</sub> 4 2D/2D Heterojunction. ACS Sustainable Chemistry and Engineering, 2019, 7, 7736-7742.	6.7	144
20	Synergistic effect of {101} crystal facet and bulk/surface oxygen vacancy ratio on the photocatalytic hydrogen production of TiO2. International Journal of Hydrogen Energy, 2019, 44, 8109-8120.	7.1	39
21	Band Positions and Photoelectrochemical Properties of Solution-Processed Silver-Substituted Cu <sub>2</sub> ZnSnS <sub>4</sub> Photocathode. ACS Applied Energy Materials, 2019, 2, 2779-2785.	5.1	44
22	Interfacial Construction of Zero-Dimensional/One-Dimensional g-C <sub>3</sub> N <sub>4</sub> Nanoparticles/TiO <sub>2</sub> Nanotube Arrays with Z-Scheme Heterostructure for Improved Photoelectrochemical Water Splitting. ACS Sustainable Chemistry and Engineering, 2019, 7, 2483-2491.	6.7	114
23	Highly efficient photocatalytic reduction of CO2 on surface-modified Ti-MCM-41 zeolite. Catalysis Today, 2019, 335, 221-227.	4.4	28
24	The effect of N-doped form on visible light photoactivity of Z-scheme g-C3N4/TiO2 photocatalyst. Applied Surface Science, 2019, 466, 268-273.	6.1	27
25	Effect of platinum dispersion on photocatalytic performance of Pt-TiO2. Journal of Nanoparticle Research, 2018, 20, 1.	1.9	18
26	Constructing a ZnIn <sub>2</sub> S <sub>4</sub> nanoparticle/MoS <sub>2</sub> -RGO nanosheet 0D/2D heterojunction for significantly enhanced visible-light photocatalytic H <sub>2</sub> production. Dalton Transactions, 2018, 47, 6800-6807.	3.3	44
27	PtNi Alloy Cocatalyst Modification of Eosin Y-Sensitized g-C3N4/GO Hybrid for Efficient Visible-Light Photocatalytic Hydrogen Evolution. Nanoscale Research Letters, 2018, 13, 33.	5.7	25
28	AgIn5S8 nanoparticles anchored on 2D layered ZnIn2S4 to form 0D/2D heterojunction for enhanced visible-light photocatalytic hydrogen evolution. Applied Catalysis B: Environmental, 2018, 227, 512-518.	20.2	129
29	Bimodal hole transport in bulk BiVO <sub>4</sub> from computation. Journal of Materials Chemistry A, 2018, 6, 3714-3723.	10.3	20
30	Adjusting the ratio of bulk single-electron-trapped oxygen vacancies/surface oxygen vacancies in TiO <sub>2</sub> for efficient photocatalytic hydrogen evolution. Catalysis Science and Technology, 2018, 8, 2809-2817.	4.1	64
31	An oxygen-vacancy-rich Z-scheme g-C3N4/Pd/TiO2 heterostructure for enhanced visible light photocatalytic performance. Applied Surface Science, 2018, 440, 432-439.	6.1	53
32	Effect of annealing ambience on the formation of surface/bulk oxygen vacancies in TiO2 for photocatalytic hydrogen evolution. Applied Surface Science, 2018, 428, 640-647.	6.1	115
33	Efficient visible-light-driven photocatalytic hydrogen production from water by using Eosin Y-sensitized novel g-C3N4/Pt/GO composites. Journal of Materials Science, 2018, 53, 774-786.	3.7	57
34	Preparation of molybdenum-doped akaganeite nano-rods and their catalytic effect on the viscosity reduction of extra heavy crude oil. Applied Surface Science, 2018, 427, 1080-1089.	6.1	19
35	New Amphiphilic Polymer with Emulsifying Capability for Extra Heavy Crude Oil. Industrial & Engineering Chemistry Research, 2018, 57, 17013-17023.	3.7	29
36	Role of Oxygen Vacancies on Oxygen Evolution Reaction Activity: β-Ga <sub>2</sub> O <sub>3</sub> as a Case Study. Chemistry of Materials, 2018, 30, 7714-7726.	6.7	43

#	Article	IF	CITATIONS
37	Spin-flip effect enhanced photocatalytic activity in Fe and single-electron-trapped oxygen vacancy co-doped TiO2. Applied Surface Science, 2018, 457, 633-643.	6.1	12
38	Interfacial oxygen vacancy layer of a Z-scheme BCN–TiO <sub>2</sub> heterostructure accelerating charge carrier transfer for visible light photocatalytic H <sub>2</sub> evolution. Catalysis Science and Technology, 2018, 8, 3629-3637.	4.1	27
39	Aquathermolysis of heavy crude oil with ferric oleate catalyst. Petroleum Science, 2018, 15, 613-624.	4.9	25
40	Solvothermal synthesis of TiO2 nanocrystals with {001} facets using titanic acid nanobelts for superior photocatalytic activity. Applied Surface Science, 2017, 391, 311-317.	6.1	30
41	Synergistic effect of surface and bulk single-electron-trapped oxygen vacancy of TiO2 in the photocatalytic reduction of CO2. Applied Catalysis B: Environmental, 2017, 206, 300-307.	20.2	374
42	Effect of reaction temperature and hydrogen donor on the Ni <sup>0</sup> @graphene-catalyzed viscosity reduction of extra heavy crude oil. Petroleum Science and Technology, 2017, 35, 196-200.	1.5	6
43	Effect of the calcination temperature on the visible light photocatalytic activity of direct contact Z-scheme g-C 3 N 4 -TiO 2 heterojunction. Applied Catalysis B: Environmental, 2017, 212, 106-114.	20.2	177
44	Remarkable enhancement in solar hydrogen generation from MoS 2 -RGO/ZnO composite photocatalyst by constructing a robust electron transport pathway. Chemical Engineering Journal, 2017, 327, 397-405.	12.7	71
45	Z-scheme BCN-TiO2 nanocomposites with oxygen vacancy for high efficiency visible light driven hydrogen production. International Journal of Hydrogen Energy, 2017, 42, 28434-28444.	7.1	37
46	Synthesis of SO4 2â^'/Zr-silicalite-1 zeolite catalysts for upgrading and visbreaking of heavy oil. Journal of Nanoparticle Research, 2017, 19, 1.	1.9	6
47	Enhanced visible light activity on direct contact Z-scheme g-C3N4-TiO2 photocatalyst. Applied Surface Science 2017 391 184-193 Enhanced Heavy Oil Recovery in Mild Conditions by <mml:math< td=""><td>6.1</td><td>240</td></mml:math<>	6.1	240
48	xmlns:mml="http://www.w3.org/1998/Math/MathML" id="M1"> <mml:mrow><mml:msup><mml:mrow><mml:msub><mml:mrow><mml:mi mathvariant="bold"&gt;S<mml:mi mathvariant="bold"&gt;O</mml:mi </mml:mi </mml:mrow><mml:mrow><mml:mn mathvariant="bold"&gt;4</mml:mn </mml:mrow></mml:msub></mml:mrow><mml:mrow><mml:mrow></mml:mrow></mml:mrow></mml:msup></mml:mrow> <td>2.7</td> <td>7</td>	2.7	7
49	Inathvaluate bold 344/Infinition/24	20.2	93
50	Photocatalytic Oxidation of Propylene on Pd-Loaded Anatase TiO2 Nanotubes Under Visible Light Irradiation. Nanoscale Research Letters, 2016, 11, 271.	5.7	12
51	Facile synthesis of a conjugation-grafted-TiO2 nanohybrid with enhanced visible-light photocatalytic properties from nanotube titanic acid precursors. Journal of Nanoparticle Research, 2016, 18, 1.	1.9	2
52	Surface heterojunction between (001) and (101) facets of ultrafine anatase TiO2 nanocrystals for highly efficient photoreduction CO2 to CH4. Applied Catalysis B: Environmental, 2016, 198, 378-388.	20.2	118
53	Effect of Different Doping Order of V and N on the Photoelectrochemical and Photocatalytic Properties of TiO <sub>2</sub> under Visible Light Irradiation from Nanotubular Titanic Acid Precursors. Journal of the Electrochemical Society, 2016, 163, H42-H47.	2.9	12
54	Enhanced Photocurrent and Photocatalytic Degradation of Methyl Orange by V-N Codoped TiO2Nanotube Arrays Cooperated with H2O2. Journal of the Electrochemical Society, 2015, 162, H557-H563.	2.9	13

#	Article	IF	CITATIONS
55	Synergistic effect of single-electron-trapped oxygen vacancies and carbon species on the visible light photocatalytic activity of carbon-modified TiO2. Materials Chemistry and Physics, 2015, 153, 117-126.	4.0	9
56	Visible light photocatalytic activities of carbon nanotube/titanic acid nanotubes derived-TiO2 composites for the degradation of methylene blue. Advanced Powder Technology, 2015, 26, 8-13.	4.1	13
57	Endowing single-electron-trapped oxygen vacancy self-modified titanium dioxide with visible-light photocatalytic activity by grafting Fe(III) nanocluster. Applied Catalysis B: Environmental, 2015, 172-173, 37-45.	20.2	30
58	Photocatalytic oxidation of propylene on La and N codoped TiO2 nanoparticles. Journal of Nanoparticle Research, 2015, 17, 1.	1.9	10
59	Magnetically Separable Fe3O4/AgBr Hybrid Materials: Highly Efficient Photocatalytic Activity and Good Stability. Nanoscale Research Letters, 2015, 10, 952.	5.7	33
60	In situ anion-exchange synthesis and photocatalytic activity of AgBr/Ag2O heterostructure. Applied Surface Science, 2015, 341, 190-195.	6.1	25
61	Enhanced photocatalytic oxidation of propylene over V-doped TiO2 photocatalyst: Reaction mechanism between V5+ and single-electron-trapped oxygen vacancy. Applied Catalysis B: Environmental, 2015, 176-177, 160-172.	20.2	78
62	Photoreduction of CO2 on TiO2/SrTiO3 Heterojunction Network Film. Nanoscale Research Letters, 2015, 10, 1054.	5.7	14
63	Enhancement of Visible-Light-Induced Photocurrent and Photocatalytic Activity of V and N Codoped TiO <sub>2</sub> Nanotube Array Films. Journal of the Electrochemical Society, 2014, 161, H416-H421.	2.9	17
64	Preparation of Cerium Modified Titanium Dioxide Nanoparticles and Investigation of Their Visible Light Photocatalytic Performance. International Journal of Photoenergy, 2014, 2014, 1-9.	2.5	11
65	Reprint of "Photocatalytic reduction of CO2 on MgO/TiO2 nanotube films― Applied Surface Science, 2014, 319, 16-20.	6.1	33
66	Enhanced photocatalytic activity of titania nanotube array films supported with highly dispersed Pt nanoparticles. Japanese Journal of Applied Physics, 2014, 53, 115505.	1.5	1
67	Preparation of Bi-doped TiO2 nanoparticles and their visible light photocatalytic performance. Chinese Journal of Catalysis, 2014, 35, 1578-1589.	14.0	30
68	Photocatalytic reduction of CO 2 on MgO/TiO 2 nanotube films. Applied Surface Science, 2014, 314, 458-463.	6.1	80
69	Self-organized vanadium and nitrogen co-doped titania nanotube arrays with enhanced photocatalytic reduction of CO2 into CH4. Nanoscale Research Letters, 2014, 9, 272.	5.7	43
70	Preparation of Ag <sub>3</sub> PO <sub>4</sub> -Loaded Carbon Nitride Nanosheets and Investigation of Their Visible Light Photocatalytic Activity. Science of Advanced Materials, 2014, 6, 2153-2158.	0.7	4
71	Preparation of Novel N-TiO2 by a Solid-State Method and Its Photocatalytic Activity. Chinese Journal of Catalysis, 2014, 32, 1430-1435.	14.0	1
72	Pseudo and true visible light photocatalytic activity of nanotube titanic acid/graphene composites. Journal of Nanoparticle Research, 2013, 15, 1.	1.9	2

#	Article	IF	CITATIONS
73	Photoelectrochemical and photocatalytic properties ofÂAg-loaded BaTiO3/TiO2 heterostructure nanotube arrays. International Journal of Hydrogen Energy, 2013, 38, 12977-12983.	7.1	32
74	Facile synthesis and enhanced visible light photocatalytic activity of N and Zr co-doped TiO2 nanostructures from nanotubular titanic acid precursors. Nanoscale Research Letters, 2013, 8, 543.	5.7	27
75	Preparation of Pd-loaded La-doped TiO2 nanotubes and investigation of their photocatalytic activity under visible light. Journal of Nanoparticle Research, 2013, 15, 1.	1.9	17
76	Preparation and characterization of Pd/N codoped TiO2 photocatalysts with high visible light photocatalytic activity. Chinese Journal of Catalysis, 2013, 34, 1418-1428.	14.0	12
77	Recoverable visible light photocatalytic activity of wide band gap nanotubular titanic acid induced by H2O2-pretreatment. Applied Catalysis B: Environmental, 2013, 138-139, 326-332.	20.2	19
78	Effect of carbon content and calcination temperature on the electrochemical performance of lithium iron phosphate/carbon composites as cathode materials for lithium-ion batteries. Advanced Powder Technology, 2013, 24, 593-598.	4.1	10
79	BaTiO3/TiO2 heterostructure nanotube arrays for improved photoelectrochemical and photocatalytic activity. Electrochimica Acta, 2013, 91, 30-35.	5.2	77
80	Nickel Titanates Hollow Shells: Nanosphere, Nanorod, and Their Photocatalytic Properties. Journal of Nanoscience and Nanotechnology, 2013, 13, 504-508.	0.9	10
81	Enhanced Visible Light Photocatalytic Activity for TiO <sub><b>2</b></sub> Nanotube Array Films by Codoping with Tungsten and Nitrogen. International Journal of Photoenergy, 2013, 2013, 1-8.	2.5	18
82	Fabrication of Mo+N-Codoped TiO <sub>2</sub> Nanotube Arrays by Anodization and Sputtering for Visible Light-Induced Photoelectrochemical and Photocatalytic Properties. Journal of Nanomaterials, 2013, 2013, 1-9.	2.7	4
83	Incorporation of Sn <sup>2+</sup> Into Titanic Acid Nanotubes and Investigation of Their Visible-Light-Responsive Photocatalytic Activity. Science of Advanced Materials, 2013, 5, 227-232.	0.7	1
84	Molybdenum and Nitrogen Co-Doped Titanium Dioxide Nanotube Arrays with Enhanced Visible Light Photocatalytic Activity. Science of Advanced Materials, 2013, 5, 535-541.	0.7	45
85	Preparation of g-C <sub>3</sub> N <sub>4</sub> /TiO <sub>2</sub> Nanocomposites and Investigation of Their Photocatalytic Activity. Science of Advanced Materials, 2013, 5, 1316-1322.	0.7	29
86	Preparation of Pt-Doped TiO <sub>2</sub> by Hydrothermal Method and Its Photocatalytic Performance under Visible Light Irradiation. Chinese Journal of Catalysis, 2013, 33, 550-556.	14.0	1
87	A new method of preparation of AgBr/TiO2 composites and investigation of their photocatalytic activity. Journal of Nanoparticle Research, 2012, 14, 1.	1.9	19
88	PHOTOCATALYTIC ACTIVITY AND PHOTOCURRENT PROPERTIES OF TIO2 NANOTUBE ARRAYS INFLUENCED BY CALCINATION TEMPERATURE AND TUBE LENGTH. Surface Review and Letters, 2012, 19, 1250023.	1.1	3
89	AgBr modified TiO2 nanotube films: highly efficient photo-degradation of methyl orange under visible light irradiation. RSC Advances, 2012, 2, 9781.	3.6	27
90	Twice heat-treating to synthesize TiO2/carbon composites with visible-light photocatalytic activity. Materials Letters, 2012, 88, 79-81.	2.6	12

#	Article	IF	CITATIONS
91	Facile synthesis and photocatalytic activity of platinum decorated TiO2â~'N : Perspective to oxygen vacancies and chemical state of dopants. Catalysis Communications, 2012, 20, 46-50.	3.3	32
92	The effect of infrared light on visible light photocatalytic activity: An intensive contrast between Pt-doped TiO2 and N-doped TiO2. Applied Catalysis B: Environmental, 2012, 113-114, 61-71.	20.2	53
93	Photoelectrochemical and photocatalytic properties of N+S co-doped TiO2 nanotube array films under visible light irradiation. Materials Chemistry and Physics, 2011, 129, 553-557.	4.0	95
94	Preparation and characterization of titanate nanotubes/carbon composites. Materials Chemistry and Physics, 2011, 130, 827-830.	4.0	5
95	Visible light active N-doped TiO2 prepared from different precursors: Origin of the visible light absorption and photoactivity. Applied Catalysis B: Environmental, 2011, 104, 268-274.	20.2	124
96	Enhanced visible light photocatalytic activity of N-doped TiO2 in relation to single-electron-trapped oxygen vacancy and doped-nitrogen. Applied Catalysis B: Environmental, 2010, 100, 84-90.	20.2	249
97	Effect of Clâ^ anions on photocatalytic decomposition of gaseous ozone over Au @ Ag/TiO2 catalyst. Research on Chemical Intermediates, 2009, 35, 817-826.	2.7	3
98	A NEW METHOD TO PREPARE THE NOVEL ANATASE <font>TiO</font> <sub>2</sub> . Surface Review and Letters, 2008, 15, 509-513.	1.1	4
99	n/p-Type changeable semiconductor TiO2 prepared from NTA. Journal of Nanoparticle Research, 2007, 9, 951-957.	1.9	36
100	Preparation and characterization of nanotube Li-Ti-O by molten salt method. Frontiers of Chemistry in China: Selected Publications From Chinese Universities, 2007, 2, 265-269.	0.4	0
101	PREPARATION OF Au-LOADED TIO2 BY PHOTOCHEMICAL DEPOSITION AND OZONE PHOTOCATALYTIC DECOMPOSITION. Surface Review and Letters, 2006, 13, 51-55.	1.1	25
102	Photo and photoelectrochemical properties of p-type low-temperature dehydrated nanotube titanic acid. Electrochemistry Communications, 2006, 8, 741-746.	4.7	31
103	Effect of photocatalytic activity of CO oxidation on Pt/TiO2 by strong interaction between Pt and TiO2 under oxidizing atmosphere. Journal of Molecular Catalysis A, 2006, 258, 83-88.	4.8	65
104	A novel N-doped TiO2 with high visible light photocatalytic activity. Journal of Molecular Catalysis A, 2006, 260, 1-3.	4.8	102
105	Microwave-assisted synthesis of potassium titanate nanowires. Materials Letters, 2006, 60, 3015-3017.	2.6	35
106	Microwave-assisted Preparation of Titanate Nanotubes. Chemistry Letters, 2005, 34, 1168-1169.	1.3	29
107	Insertion of Platinum Oxide into Nanotube of Sodium Titanate. Journal of Nanoparticle Research, 2005, 7, 681-683.	1.9	5
108	EFFECT OF Au DEPOSITION ON PHOTOCATALYTIC ACTIVITY OF ZnO NANOPARTICLES FOR CO OXIDATION. Surface Review and Letters, 2005, 12, 749-752.	1.1	6

#	Article	IF	CITATIONS
109	Effect of annealing temperature on morphology, structure and photocatalytic behavior of nanotubed H2Ti2O4(OH)2. Journal of Molecular Catalysis A, 2004, 217, 203-210.	4.8	308
110	Study on ESR and inter-related properties of vacuum-dehydrated nanotubed titanic acid. Journal of Solid State Chemistry, 2004, 177, 1365-1371.	2.9	123
111	Study on composition, structure and formation process of nanotube Na2Ti2O4(OH)2. Dalton Transactions, 2003, , 3898.	3.3	428
112	Mechnism of Photocatalytic Oxidation of Formaldehyde. Wuli Huaxue Xuebao/ Acta Physico - Chimica Sinica, 2001, 17, 278-281.	4.9	9
113	A study of the photocatalytic oxidation of formaldehyde on Pt/Fe2O3/TiO2. Journal of Photochemistry and Photobiology A: Chemistry, 2000, 137, 197-202.	3.9	96
114	Kinetic effect in the size-control of CdS nanoparticles. Science in China Series B: Chemistry, 1999, 42, 631-638.	0.8	1
115	Study on the structure and tribological properties of surface-modified Cu nanoparticles. Materials Research Bulletin, 1999, 34, 1361-1367.	5.2	148
116	Electrocatalysis and flow-injection analysis of hydrogen peroxide at a chemically modified electrode. Analytica Chimica Acta, 1992, 259, 211-218.	5.4	36